Archives of Hydro-Engineering and Environmental Mechanics
Vol. 54 (2007), No. 2, pp. 77–94

Loads on an Off-Shore Structure due to an Ice Floe Impact

Ryszard Staroszczyk

Institute of Hydro-Engineering, Polish Academy of Sciences, ul. Waryńskiego 17,
71-310 Szczecin, Poland, e-mail: rstar@ibwpan.gda.pl

(Received November 23, 2006; revised February 14, 2007)

Abstract

In the paper, the problem of dynamic impact of a floating ice sheet at an off-shore structure is considered. It is assumed that during an interaction event the dominant mechanism is the brittle fracture of ice at the ice–structure interface, that is, elastic and creep effects in ice are ignored. Since in natural conditions the edge of floating ice is usually irregular, the contact between a floe and an engineering object is imperfect. Thus, at any one time, the failure of ice occurs only in a number of small zones along a structure wall, leading to a highly irregular variation of forces exerted on the structure during the impact process. It is supposed in the analysis that the successive small-scale fracture events at the contact surface occur at random, and all these small-scale events take place independently of each other. An off-shore structure is modelled as a fixed and rigid circular cylinder with vertical walls. For an adopted geometry of the ice sheet, its initial horizontal velocity, and the variety of parameters describing the limit failure stresses in ice, the history of total loads sustained by the structure and the floe velocity variation are illustrated for a typical impact event. Furthermore, probability distributions for maximum impact forces exerted on the structure, depending on the floe size, its thickness and initial velocity, are determined.

Key words: floating ice, off-shore structure, dynamic impact, brittle fracture

Notations

A, A_0 – ice–structure contact area, reference area,
b – discrete ice element size,
F_x, F_y – components of total force sustained by a structure,
h – ice floe thickness,
m – floe mass,
r_0, R_0 – cylinder radius, floe radius,
t – time,
v – floe velocity,
V_0 – initial floe velocity,
x – ice penetration distance,
β – ice fracture strength scale dependance parameter,

Δ – critical displacement,
ε_f – critical failure strain,
σ_c – ice clearing stress,
σ_f – ice failure stress,
σ_f^* – normalized ice fracture strength.

1. Introduction

When a hydro-engineering structure is surrounded by a compact cover of floating ice and starts to interact with it, a variety of deformation mechanisms in ice can be observed. At the beginning of an interaction process elastic strains develop in ice, but these are very small in magnitude compared to other modes of deformation in this material and therefore are usually neglected in the analysis. If the ice is initially in more or less good contact with the structure walls (is adfrozen to them) and the forces (wind and/or water currents) driving the ice cover onto the object change slowly, then the material deforms by creep, in a continuous, or ductile, way. A number of various approaches have been pursued to describe this type of material behaviour. Most notably, these include the application of non-linearly viscous (Smith 1983, Overland and Pease 1988, Morland and Staroszczyk 1998, Staroszczyk 2005) or viscous-plastic rheological models (Hibler 1979, Ip et al 1991, Tremblay 1999, Staroszczyk 2006). Further increase in strains, strain-rates and stresses in ice leads to the next phase of the ice deformation, in which cracks develop and subsequently propagate in the medium, giving rise to the brittle behaviour of ice. Typically, sea ice undergoes a transition from ductile to brittle behaviour when either compressive stresses exceed the magnitude of about 5 MPa, or strains exceed about 0.01, or strain-rates reach the level of 10^{-4} to 10^{-3} s^{-1} (Hawkes and Mellor 1972, Sanderson 1988). During this creep-to-brittle transition phase the loads exerted by ice on the structure attain their maximum or near-maximum values; further increase in the ice deformation and velocity usually does not increase the respective forces. However, when the strains and strain-rates grow further, the cracks in ice begin to spread out quickly through the medium, and the material starts to fail by brittle fracture. Since most often the failure of ice takes place only at a number of relatively small parts of the ice–structure interface, the loads exerted on the object during this stage show a highly irregular variation in time, with a number of characteristic sharp spikes appearing at irregular time intervals. Peak forces experienced by the structure during this phase are usually smaller than those occurring during the ductile-to-brittle transition. However, if the interaction time is sufficiently long, then there is an increasing probability that subsequent failure peaks may exceed the transition peak loading.

This paper deals with the problem in which an ice floe impacts dynamically at an off-shore structure. In such a situation, due to relatively high velocities of the floe and high deformation-rates occurring in ice from the moment when the

first contact between the structure and the floe has been established, the behaviour of ice is essentially brittle in nature. Indeed, there is little evidence of continuous behaviour of ice in the vicinity of off-shore structures in Arctic seas; rather, what is commonly observed in the field, is a multitude of broken ice blocks of various shapes and sizes surrounding engineering objects (Sanderson 1988, Jordaan 2001). Therefore, in this analysis of the ice floe impact problem it is assumed that during the ice–structure interaction the material fails by brittle fracture, and hence other types of ice behaviour are disregarded.

The description of the ice fracture mechanism is difficult, and requires the knowledge of advanced methods of both experimental and theoretical mechanics. A number of theories, with increasing degrees of generality, have been developed over the past two decades to describe the mechanism of brittle failure of ice (Ashby and Hallam 1986, Sjölind 1987, Nixon 1996, Pralong et al 2006). Unfortunately, despite all their merits, these formulations seem to be too complex to be effectively implemented into realistic, engineering applications, as they involve many material parameters that cannot be satisfactorily determined for the types of sea-ice encountered in natural conditions. For this reason, a very simple method is proposed here, in which the mechanism of ice failure is described, essentially, by only three parameters: (1) axial compressive failure stress, (2) an associated axial strain at which the fracture occurs, and (3) ice clearing axial stress, which is a stress occurring in already fractured blocks of ice. Undoubtedly, such an approximation ignores many interesting local processes taking place in ice during its brittle fracture. However, this study is primarily focused on the determination of total net forces that the ice floe exerts on the structure, thus all small-scale phenomena occurring in the material near the ice–structure interface are deemed unimportant for the purposes of the present analysis.

In this work, an engineering structure is modelled as a rigid, circular in plane cylinder with vertical walls. An ice floe that hits the structure is treated as a compact slab of thickness constant along the contact surface. The interaction between the floe and the object is assumed to occur, at any given time, at a number of small zones, with local fractures taking place non-simultaneously in different parts of the contact interface. In this way, the non-perfectness of the ice–structure contact and the material non-homogeneities are accounted for. The local failure of ice at each small zone is supposed to occur independently of the other zones, and all these independent local fracture events are treated as separate random processes. Accordingly, the total load sustained by the structure is determined as a statistical sum of individual loads coming from all the small contact zones. Hence, assuming the floe dimension (or mass) and its initial velocity, probability distributions of maximum total contact forces occurring during the collision process are calculated by simulating numerically a large number of single impact events. In particular, the probability distributions showing the dependence of peak interaction forces on the floe thickness, its size and its initial velocity are determined. In addition, the time

variations of the total impact force, the floe velocity, and the distance travelled by the floe during a typical impact event are illustrated.

2. Non-Simultaneous Fracture of Ice

The problem considered is depicted in Fig. 1. An ice floe, initially at some distance from a rigid structure, driven by wind and/or water current drag forces, is moving towards the object at the horizontal velocity V_0, carrying some amount of kinetic energy. After arriving at the structure at time t_0 and establishing contact with its walls, the ice starts to fail at locations at which the magnitudes of local contact stresses reach the brittle failure strength of ice. As the ice is progressively crushed, and also piled up or sunk near the structure, the initial energy of the impacting floe is dissipated, and the floe velocity, $v(t)$, with t denoting time elapsed from the instant t_0, gradually decreases until the ice sheet comes to rest.

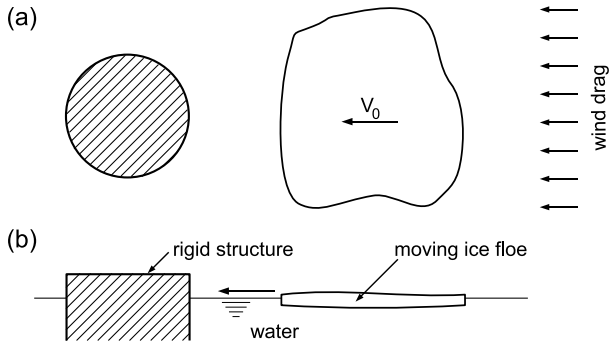

Fig. 1. Definition of the problem: (a) planar and (b) cross-sectional views

Due to the geometry of the ice leading edge which in real field conditions is commonly quite irregular in shape, both in planar view and across the ice depth, the contact between the floe and the structure wall is most unlikely to take place over the entire possible interface between the ice and the object (see Fig. 2a). Further, once the interaction has been initiated and the ice starts to fail, broken blocks of different size and shape are formed in a chaotic fashion. The observed characteristic size of such fractured fragments is of the order of the floe thickness; for very thick, multi-year ice of the thickness of several metres, this size is of the order of about 1 m (Sanderson 1988). All these separate ice blocks are being crushed at the structure wall independently of one another, in a series of local failure events which can be regarded as a random process. Hence, the failure of the ice occurs in a non-simultaneous manner, as different ice fragments fail at different times at different small-area zones at the interface surface. At any one such small zone, the ice fragments are supposed to arrive and fail one by one: as one fragment fails and the debris is cleared by the process of ice piling up or sinking, another

ice fragment arrives immediately to start its interaction with the wall and to fail after some time, etc. In order to model such a complex interaction phenomenon, I apply, and refine, a method originally proposed by Ashby and Hallam (1986) and subsequently followed by Sanderson (1988). In this method, the floe is treated as a collection of regular in shape and independent cells, as shown in Figs. 2b and 2c. Each discrete cell has the same size, and is a square of dimensions $b \times b$ in the horizontal plane and has a depth h equal to the floe thickness. The dimension b corresponds to the above-mentioned characteristic size of fractured ice blocks and is chosen to be close to h (provided that geometric features of the problem under consideration enable this). As a particular cell starts to interact with the structure (Fig. 2c), it is assumed that it fails (that is, the axial stress component normal to the contact surface reaches the fracture strength of ice) when the whole discrete element is advanced by a distance Δ; the latter parameter representing a critical displacement at which the crushing of ice occurs.

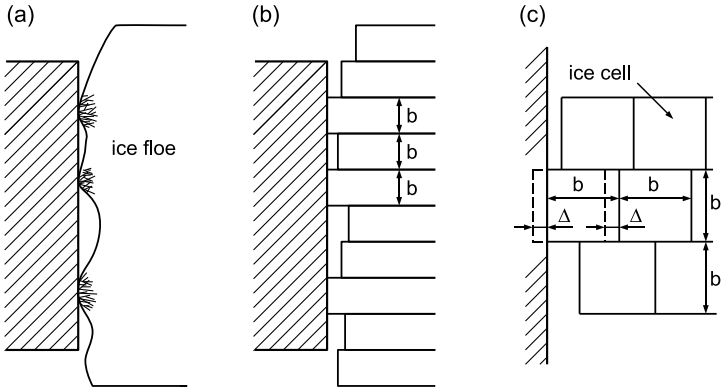

Fig. 2. (a) Imperfect contact between an ice floe and a structure wall, (b) problem idealization, (c) detailed view and definitions

The history of loading experienced by a discrete zone at the contact interface, as successive ice cells arrive and fail there, is illustrated in Fig. 3. When an ice cell comes to the rigid wall and then moves by a distance Δ, the contact stress is assumed to grow in a linear manner from zero to its peak value, equal to the ice fracture strength, σ_f. Next, immediately after the failure of ice, the contact stress drops sharply to a much lower level, σ_c, which is a stress in ice caused by forces which are needed to clear the debris formed during failure (that is, to move the fractured ice fragments up or down, since the debris cannot be cleared by pushing it aside, in the direction lateral to the impact direction). This clearing stress is supposed to remain constant until the time when the next ice block arrives at the wall and starts to fail, rising the stress gradually to the σ_f level again, etc. The failure and clearing stresses, σ_f and σ_c, for different ice cells are assumed to have different magnitudes, in order to reflect a stochastic character of the fracture mechanism and an associated

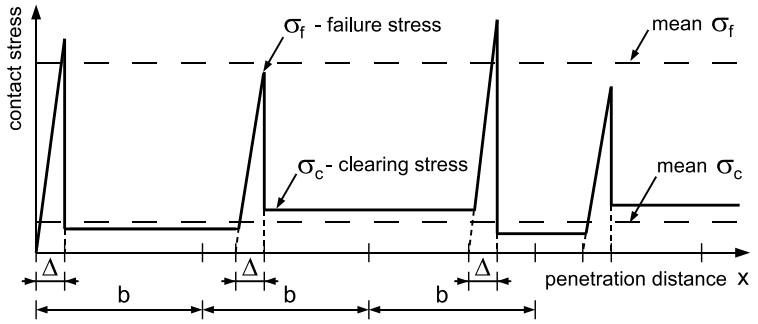

Fig. 3. Contact stress history for a single discrete zone

statistical scatter in available empirical data. The respective mean values of σ_f and σ_c are illustrated in the figure by the two horizontal dashed lines. The variations of σ_f and σ_c about their mean values are supposed to follow the normal distribution. Moreover, the distance between consecutive failure stress peaks is not uniform, but also varies in a stochastic manner; in such a way the randomness of an individual ice block size is accounted for. In the model it is assumed that the average distance separating two successive failure stress peaks is equal to b – the average size of a fractured block. Further, it is supposed there is an equal probability of a stress peak to lie anywhere within a given stretch of length b (that is, a uniform probability distribution function is used).

The model for the mechanism of the ice–structure interaction, as described above, is based on three main parameters: the stress magnitudes σ_f and σ_c (their mean values and statistical variation) and the critical displacement Δ at which an ice element of length b fails. The latter parameter will be expressed by means of a critical axial strain, ε_f, at which brittle fracture occurs.

The most significant of the above three parameters, with regard to the magnitudes of forces exerted by impacting ice on a structure, is the failure stress level σ_f, equal to the brittle fracture strength of ice. It is well known that fracture mechanisms exhibit pronounced scale-dependence, and ice is no exception. Hence, the stress under which a given sample of ice fails in a brittle way strongly depends on its geometrical dimensions, as well as the size, shape and distribution of flaws and cracks in the material. There is a host of empirical data, obtained from both small-scale laboratory and large-scale field measurements, which show how the ice peak failure stress is related to the contact area on which the stress is applied. These data, covering the range of scales varying from square centimetres to even square kilometres, have been collected, and presented in so-called *pressure-area diagrams*, in the book by Sanderson (1988). It follows from these diagrams that the compressive failure strength of ice decreases with increasing contact area, A, with a functional dependence expressed by

$$\sigma_f \propto A^{-\beta}, \tag{1}$$

where the symbol '$\propto$' means 'proportional to'. There is some discussion in the literature on the subject, concerning the most appropriate value of the parameter β in the above power law. Generally, it is accepted that β takes a value from the range 1/4 to 1/2, with the lower limit value for smaller scales ($A \lesssim 0.1$ m^2), and the upper limit value for larger scales ($A \gtrsim 10^3$ m^2). In the model proposed here, the value $\beta = 1/4$ is adopted, which has been derived by Palmer and Sanderson (1991) and Xu et al (2004) on the basis of a fractal analysis of the size distribution of fragmented sea ice. Hence, the ice size effect on the failure strength is expressed in the following, normalized, form

$$\sigma_f = \sigma_f^* \left(\frac{A}{A_0} \right)^{-1/4}, \tag{2}$$

where A_0 is a reference contact area, assumed here to be equal to 1 m^2, and σ_f^* is a normalized ice failure strength (that is, that corresponding to A_0). Xu et al (2004) suggested a value of $\sigma_f^* = 1.66$ MPa, as the one providing the best fit to the available empirical data. The latter value of β is particularly suitable for the case of contact areas of the order of 1 m^2. The failure strength defined by equation (2) represents its mean value. The experimental data for sea ice, however, show a significant statistical scatter. Sanderson (1988) carried out some detailed statistical calculations for the Arctic sea ice and found that the variation coefficient (the ratio of the standard deviation to the mean value) of the data for first-year ice is as high as about 45%, and for multi-year ice it is about 65%. In this work, as we are concerned with rather thin first-year ice, the variation coefficient equal to 50% is adopted to describe the scatter in possible values of σ_f^*. Moreover, Sanderson (1988) indicated that the probability distribution of experimental data for σ_f^* is approximately normal, and, therefore, such a type of distribution will be used in the numerical simulations.

While the failure strength of ice, σ_f, is relatively well identified and reliable empirical data sets are readily available, the magnitude of the ice clearing stress, σ_c, the other parameter in the model, is much more difficult to identify, since – as far as I am aware – no measurements of this quantity have been carried out yet during real impact events. Due to the lack of the results obtained directly in situ, a few attempts have been made by different authors, for instance Sanderson (1988), to estimate the ice clearing stresses indirectly, by purely theoretical considerations. To this end, the work done against gravity, required to rise or sink ice fragments after their failure, is calculated and compared to the work done by the forces in impacting ice. In this way the stress levels during clearing the ice post-failure debris can be determined, and it turns out that so obtained stresses are about two orders of magnitude smaller than the typical failure stresses. In order to make allowance for additional forces that can develop in ice to overcome frictional resistance of the failed material, as well as to account for dynamic effects, some numerical factors can be introduced in the analysis to increase the magnitude of the possible clearing stress. Yet, these

stresses will be appreciably smaller compared to the failure stresses. Sanderson (1988) proposed the value of 0.05 MPa for σ_c, but this was for multi-year ice of 10 m thickness. For much thinner ice floes considered in this work, a lower value for the clearing stress is adopted, namely 0.02 MPa as its mean value, together with a 50% variation coefficient, in order to describe the scatter of empirical data – the same value of the variation coefficient as that adopted above for the failure stress.

The third key parameter used in the proposed ice floe failure model is the critical strain ε_f, developing during the process of brittle crushing of ice, and determining the critical axial displacement Δ (see Fig. 3) through the relation $\Delta = \varepsilon_f b$. There is some experimental evidence regarding the strain magnitudes at which ice fractures, but this is limited to small-scale laboratory tests on fresh-water ice samples, and thus has little relevance to real large-scale field conditions. Therefore, as in the above case of σ_c, the value of the critical strain ε_f has been inferred indirectly, by some theoretical argument (Sanderson 1988). The latter author presents two examples, in one he assumed $\varepsilon_f = 0.02$, and in the other $\varepsilon_f = 0.05$, both values for thick, multi-year ice. In the present analysis the lower value is adopted, that is $\varepsilon_f = 0.02$, in belief that pre-failure strains that develop in young, thin, and therefore relatively homogeneous ice are much smaller than those occurring in multi-year, thick, and hence highly heterogenous ice. For comparison, strains measured in laboratory at failure of fresh-water ice, depending on strain-rates and stress regimes applied, have the values ranging from 0.002 to 0.007 (Schulson and Gratz 1999, Iliescu and Schulson 2002).

3. Numerical Method

Let the direction of the floe movement be defined by an axis x, with the x-coordinate measuring a distance between the floe and the structure. Assume that $x = 0$ at the time of first contact, taking place at $t = t_0$, and x grows as the ice is progressively penetrated. Hence, the x-coordinate denotes the ice penetration distance, shown in Fig. 3.

The numerical simulation of an impact event, based on the assumptions and approximations presented above, proceeds in the following steps:

1. Given the initial geometry of an ice floe, its in-plane dimensions and a mean thickness h, the ice sheet is discretized in the way shown in Fig. 2, by choosing the ice cell size b of a magnitude close to h. Also the floe mass, m, is evaluated (in the model, the effect of the added mass of underlying water is neglected).
2. For each discrete contact zone at the ice–structure interface, a separate stochastic realization of loading, as illustrated in Fig. 3, with the values of the failure and clearing stress, as well as the distance between consecutive failure stress peaks, randomized about their mean values, is prepared. For this purpose, standard random number generators for the uniform and normal probability distributions are used.

3. At each calculation step, for $t > t_0$, the floe is advanced by a small increment δx, chosen to be a fraction (one-tenth or one-twentieth) of the critical displacement $\Delta = \varepsilon_f b$. For the current value of x, a local contact stress, obtained from the respective realization of loading, is determined for each discrete zone, and all these local stresses, multiplied by the respective local contact areas, are summed together to yield a total impact force, F, at given x.
4. Assuming that during a given displacement step k ($k = 1, 2, 3, \ldots$) the interaction force, F_k, is constant, the total work done by this force over the distance δx is $F_k \delta x$. Equating that work with the amount of the total kinetic energy of the floe lost due to the decrease in its velocity from the value of v_{k-1} to v_k, the latter can be evaluated from the relation

$$v_k^2 = v_{k-1}^2 - \frac{2F_k}{m}\,\delta x, \quad k = 1, 2, 3, \ldots, \quad v_0 = v(t_0) = v(x = 0) = V_0. \tag{3}$$

5. Assuming a linear variation of the floe velocity at each step, the time which elapsed during the advance of the floe at the k-th step, denoted by $(\delta t)_k$, is calculated from the formula

$$(\delta t)_k = \frac{2\,\delta x}{v_{k-1} + v_k}\,. \tag{4}$$

All the time increments, added up over all preceding displacement steps, give the current value of time t elapsed since the beginning of the interaction process.

The procedure outlined above yields time histories of the total interaction force F, the floe velocity v, and the penetration distance x for one particular stochastic realization of an impact event. For each realization, a magnitude of the maximum force F occurring during an event is found, and then, by simulating a large number of realizations, probability distributions for the peak ice impact loads F are determined.

4. Results of Simulations

The model presented in the two preceding sections has been applied to simulate ice–structure dynamic interaction events of the geometries shown in Fig. 4. The basic configuration used in the computations is depicted in Fig. 4a, showing a cylindrical structure of radius r_0 impacted by a circular floe of radius R_0 and average thickness h, moving towards the structure with velocity $v(t)$. Strictly, only the geometry of the leading floe edge which can come in direct contact with the structure may play a role, otherwise the planar shape of the floe is irrelevant (since it is the mass of ice which matters). To examine the effect of the geometry of the impacting floe edge on the peak forces exerted on the structure, the interaction configuration shown in Fig. 4b has also been considered, in which the projection

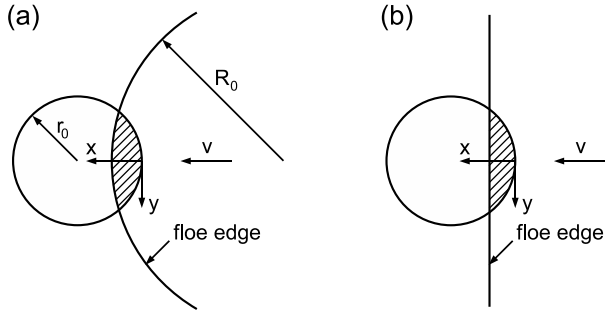

Fig. 4. Cylindrical structure of radius r_0 in contact (a) with a floe of radius R_0, (b) with a straight-edged floe. The hatched areas show the regions of ice penetrated by the structure

of the leading floe edge on the horizontal plane is a straight line normal to the ice movement direction.

The simulations have been carried out for a vertically-sided circular cylinder of radius 10 m. The main purpose was to investigate the influence of the floes initial velocity and size on the characteristics of the total forces exerted on the object. Hence, the initial ice velocity, V_0, was varied within the range 0.2 to 0.5 m s^{-1}. The latter, higher value can be regarded as a typical ice floe speed occurring in the Arctic during high wind seasons (Sanderson 1988). The ice thickness, h, was assumed to range from 0.2 to 0.5 m, pertaining to young, one-year ice. Unless otherwise stated, interaction with a circular floe of radius $R_0 = 100$ m was simulated. As discussed earlier in Section 2, the following values of the parameters used in the proposed ice fracture model were adopted: $\sigma_f^* = 1.66$ MPa, $\sigma_c = 0.02$ MPa, $\varepsilon_f = 0.02$. The ice density (needed to determine the total mass of the floe) was taken as 900 kg m^{-3}. All probability distributions presented further in this Section have been obtained by running the model repeatedly 10 000 times (that is, impact events).

Fig. 5 illustrates typical time histories of the total force acting on the cylinder along the direction of the floe advance, $F_x(t)$, the flow velocity, $v(t)$, and the ice penetration distance, $x(t)$. The results have been obtained for a floe of thickness 0.5 m, moving towards the structure at a velocity of 0.5 m s^{-1}. For this particular realization, the impact lasts nearly 25 seconds, the ice moves a distance of 6.8 m (roughly 2/3 of the cylinder radius) before it comes to rest, and the peak forces exerted on the structure have magnitudes close to 1.6 MN. While the simulated variation of the total loading is, as has been anticipated, highly irregular, the velocity of the floe, and in particular, its position against the cylinder wall, vary in a relatively smooth manner. At first sight, it might seem surprising that such highly irregular variation of the interaction forces, suggesting the presence of dynamic effects in the system, is not reflected in the plots for $v(t)$ and $x(t)$. However, each peak force, for the input parameters (ε_f, $b = h$ and V_0) adopted, acts over an average time period of about 1/25 s. Therefore, the changes in floe velocity and position occurring over

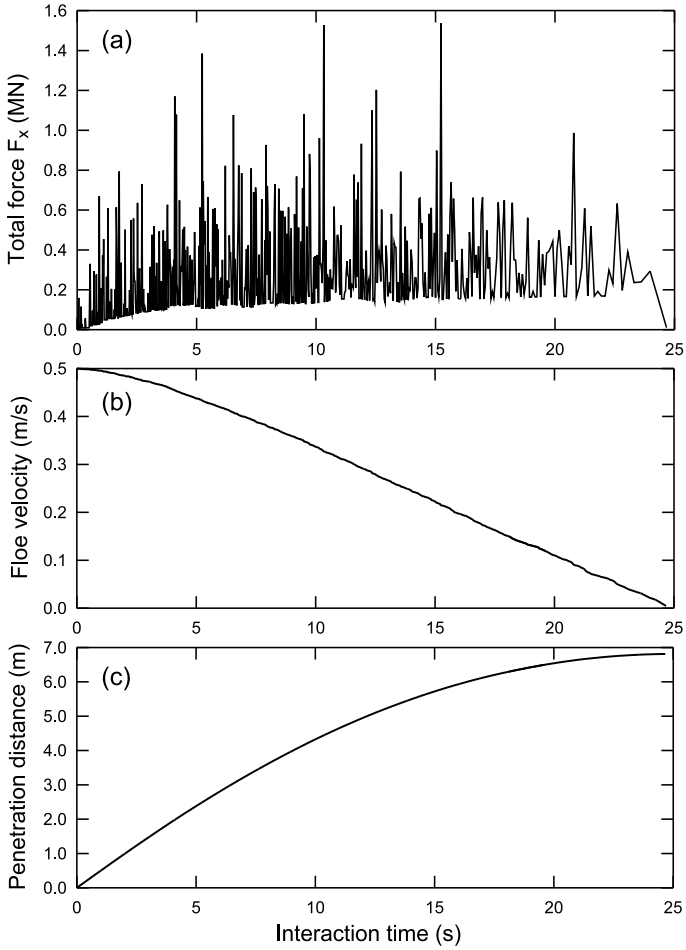

Fig. 5. Typical histories of (a) the total force F_x, (b) the floe velocity and (c) the ice penetration distance during an impact event, for the floe thickness $h = 0.5$ m and its initial velocity $V_0 = 0.5$ m s^{-1}

such short time intervals cannot be discerned on the time scales used in the plots. It is also worth noting that the force peaks of largest magnitudes gradually increase as the collision proceeds. This is because the ice–structure contact area widens with the time of interaction, hence there is an increasing number of local zones at which ice can potentially fail (that is, there is an increasing number of local contact forces which, at a particular time, can potentially contribute to the total ice floe–structure interaction force). However, although such an increase in the maximum loads with elapsed time is quite a common feature, by no means – due to the random character of the process – can it be treated as a general rule.

The results demonstrated in Fig. 5 refer to a single impact event. Due to the intrinsic randomness of the mechanism under investigation, and hence a small re-

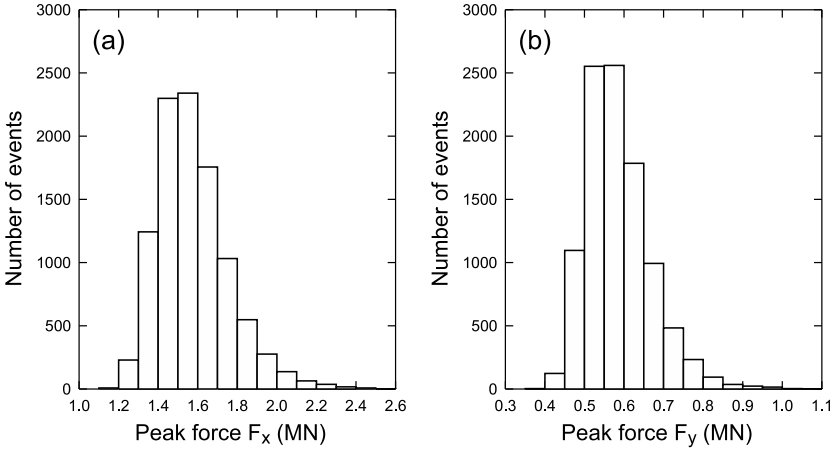

Fig. 6. Histograms of peak ice impact forces F_x and F_y obtained by simulating 10 000 events, for the floe thickness $h = 0.5$ m and its initial velocity $V_0 = 0.5$ m s^{-1}

peatability of the results obtained for a single event, it is necessary to perform a series of simulations, the longer the better, in order to infer information of a more general use. For this purpose, a series of 10 000 impact events has been simulated, adopting the same set of input parameters relating to the floe as those used in the previous figure. As in engineering practice we are usually most interested in the magnitudes of forces exerted on the structure, Fig. 6 presents histograms showing the frequency distributions of peak impact loads – the components F_x and F_y acting, respectively, along the axes x and y, as shown in Fig. 4. One can immediately notice that the peak loads acting in the lateral direction, F_y, can attain quite large magnitudes compared to the loads F_x along the floe movement direction. For floe velocity $V_0 = 0.5$ m s^{-1} and ice thickness $h = 0.5$ m, the average values of the peak load components are $\overline{F}_x = 1.58$ MN and $\overline{F}_y = 0.59$ MN (with respective standard deviations 0.18 MN and 0.08 MN), so that the mean lateral peak force equals nearly 2/5 of the mean longitudinal component. Similar ratios of the F_y to F_x components have been obtained for other combinations of the floe parameters. It can be observed in the histograms that the peak load distributions are not symmetric about their mean values, hence they cannot be approximated by the normal distribution. The shape of the frequency histograms suggests the Poisson, or, possibly, the Weibull distribution. The latter type of the probability density distribution often occurs in fracture mechanics, and with regard to ice fracture phenomena it has already appeared in a number of analyses, for instance by Kim and Shyam Sunder (1997) and Kamio et al (2003).

The diagrams in Figs. 7 to 10 present density probability distributions of peak forces exerted by impacting ice. These figures illustrate the influence of the floe velocity, its thickness, planar size, and the value of the model parameter ε_f, on the magnitude of the total contact force F_x and the statistics of its occurrence.

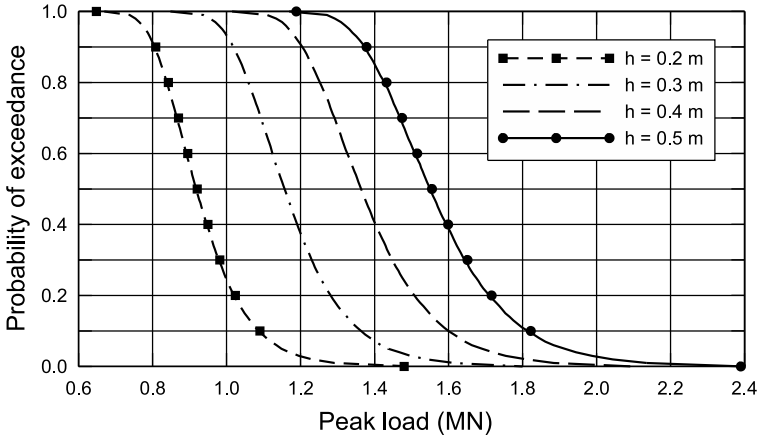

Fig. 7. Exceedance probability distributions of peak impact loads exerted on the structure for the initial floe velocity $V_0 = 0.5$ m s^{-1} and different floe thicknesses h. Compared are the results for circular and straight-edged floes

The plots are arranged in such a way that for each value of the load F_x obtained from the simulations, the probability that this particular value will be exceeded is shown. Fig. 7 demonstrates the effect of the floe thickness h on the exceedance probabilities of the total impact loads. Accordingly, for different values of h, with the ice velocity V_0 and the plane floe dimensions kept unchanged, the respective probability distributions are plotted. Moreover, the effect of the impacting floe geometry is illustrated by considering the two configurations depicted in Fig. 4, namely (a) the circular floe of radius $R_0 = 100$ m and (b) the straight-edged floe of the same mass as the round one. The results for the circular floe are shown by the four lines for $h = 0.2$, 0.3, 0.4 and 0.5 m respectively, and the results for the floe with the straight leading edge are shown by the squares ($h = 0.2$ m) and the circles ($h = 0.5$ m). It is seen that the influence of the floe edge geometry on the load probability distributions is negligibly small – the maximum relative discrepancies are of the order of 1%. On the other hand, the influence of the ice thickness on the impact load magnitudes is, obviously, significant. However, the total loads sustained by the cylinder are not roughly proportional to the ice thickness, as could be expected at first sight, due to two factors. First, the thicker floe has smaller fracture strength σ_f^* than its thinner counterpart, as is described in Section 2, and in particular is quantified by equation (2). And second, the thicker floe, due to its larger mass, interacts with the structure for a longer time, which enhances chances for larger peak forces to occur during an impact event.

Fig. 8 shows the exceedance curves for peak loads F_x as a function of the initial velocity of ice, V_0, with the other problem parameters (h, R_0 and ε_f) kept constant. Hence, for the velocities V_0 ranging from 0.2 to 0.5 m s^{-1} and the ice 0.5 m thick, the probability distributions for F_x are displayed. It can be noted that, despite

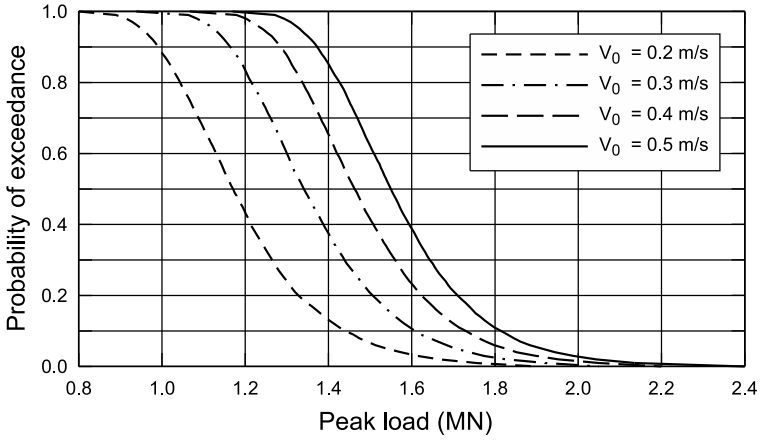

Fig. 8. Exceedance probability distributions of peak impact loads exerted on the structure for the floe thickness $h = 0.5$ m and different initial floe velocities V_0

a significant increase in the total kinetic energy of a floe, which is 6.25 times larger in the case of the velocity changed from 0.2 (the short dashed line) to 0.5 m s^{-1} (the solid line), the magnitudes of the total loads, at the same probability of exceedance, increase merely by a factor of about 1.25 to 1.4. This increase in impact loading has two sources. Firstly, the ice penetration distance is larger for the faster moving floe, hence – for the adopted circular geometry of the structure – the maximum total contact area is larger. Secondly, an increase in the average time of an impact event (changing from 15.7 s for $V_0 = 0.2$ m s^{-1} to 24.6 s for $V_0 = 0.5$ m s^{-1}) increases the likelihood of larger peak loads appearing during a collision event.

In Fig. 9 the floe size effect on the exceedance probabilities of the peak impact forces is demonstrated. That is, the results of simulations carried out for circular floes of radii varying between 50 and 200 m are plotted. In some way, the character of the exceedance curves resembles that shown in the previous diagram. Although the kinetic energy grows quite considerably with increasing floe radius (by a factor of 16 between the smallest and the largest floes considered), this translates to much smaller variations of the peak load magnitudes occurring with the same probability of exceedance. The reasons for the peak loads increase are again twofold: an increase in the total contact area, and an increase in the impact duration time.

The previous three diagrams illustrated the effects of the floe geometry (its thickness, planar size and leading edge shape) and the floe initial velocity on the probability distributions of the interaction force. In Fig. 10 we show how the magnitude of the critical strain, ε_f, affects the resulting load distributions. The latter parameter is one of the three main parameters of the impact model presented, and the one which is the most difficult to be realistically estimated. Hence, the exceedance curves for the peak impact forces are plotted for a set of different values of ε_f, including the value 0.02 used in all previous simulations. It is seen in the

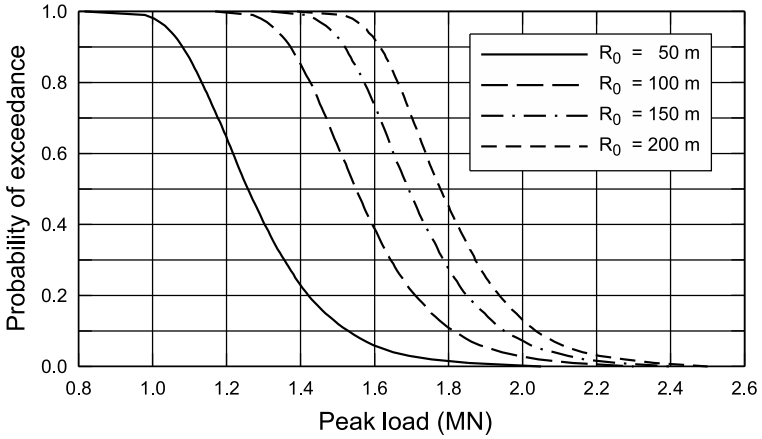

Fig. 9. Exceedance probability distributions of peak impact loads for the initial floe velocity $V_0 = 0.5$ m s^{-1}, ice thickness $h = 0.5$ m, and different floe radii R_0

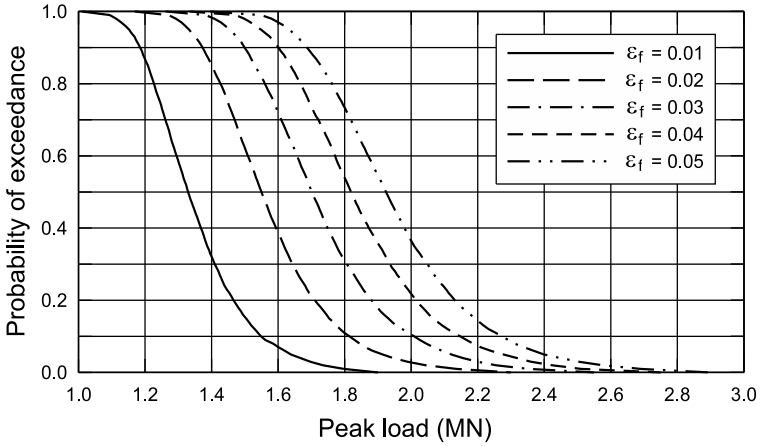

Fig. 10. Exceedance probability distributions of peak impact loads for the initial floe velocity $V_0 = 0.5$ m s^{-1}, ice thickness $h = 0.5$ m, and different values of the critical strain ε_f

figure that the magnitude of the critical failure strain has a significant effect on the theoretical predictions of the model, since a change in ε_f from 0.01 to 0.05 gives rise to an increase in the magnitudes of total forces occurring with the same exceedance probability, ranging from about 30% for lower values of probabilities to about 50% for higher ones.

Finally, Table 1 presents mean values, together with respective standard deviations, of the impact duration time T, and the maximum distance X travelled by the ice floe during a collision event, that is, between the time the ice floe hits the cylinder wall until it ultimately comes to rest. The table lists the result obtained for several sets of parameters used in the simulations whose results are shown in the preceding plots. For most of the parameter combinations considered, the ice

Table 1. Mean values of impact time T and total penetration distance X, together with their standard deviations (given after the sign ±) for different combinations of the initial floe velocity V_0, thickness h, floe radius R_0, and critical strain ε_f, for a cylindrical structure of radius $r_0 = 10$ m

V_0 [m/s]	h [m]	R_0 [m]	ε_f	T [s]	X [m]
0.5	0.5	100	0.02	24.6 ± 0.6	6.9 ± 0.1
0.5	0.2	100	0.02	19.6 ± 0.6	5.5 ± 0.1
0.2	0.5	100	0.02	15.7 ± 0.9	1.8 ± 0.1
0.5	0.5	50	0.02	8.8 ± 0.4	2.6 ± 0.1
0.5	0.5	200	0.02	86.2 ± 1.1	22.4 ± 0.2
0.5	0.5	100	0.01	32.0 ± 0.6	8.8 ± 0.1
0.5	0.5	100	0.05	15.3 ± 0.6	4.4 ± 0.1

penetration distance X does not exceed the cylinder radius, except the cases of very large floes. Also a pronounced effect of the critical strain parameter ε_f on the values of T and X (much larger an effect than on the magnitudes of the total impact forces) can be noted. It might seem somewhat unexpected that the values of the standard deviations for T and X are relatively small. However, one should bear in mind that the parameters describing the ice floe velocity, as well as its thickness and radius have not been treated in the simulations as random variables – the randomization has concerned only the parameters directly related to the mechanism of ice fracture. Hence, the total kinetic energy of the impacting floe has not been randomized, and this is the quantity which is the most important factor in terms of the total impact time and the ice penetration distance; the statistical scatter in the parameters describing the ice fracture strength σ_f^* and the critical axial strain ε_f has an effect mainly on the statistical variation in the magnitudes of single contact force peaks.

5. Conclusions

The mechanical model for the ice floe impact problem has been constructed by assuming that the dominant mechanism occurring during an ice–structure interaction event is the brittle fracture of ice at a structure wall. The model incorporates such features as imperfectness of the floe–structure contact and randomness of the ice failure processes taking place at the structure wall. Hence, the failure stresses in ice are assumed to be random variables, with their magnitudes varying significantly about the mean values to reflect large scatter in available empirical data on the compressive strength of ice. Further, the randomness of the dimensions of fragmented ice blocks that interact with the structure is considered. The results obtained by simulating a large number of single impact events provide probability distributions of the total forces exerted on the structure, in particular, the effects of the floe dimensions and its initial velocity have been investigated.

There is no doubt that the proposed model, which, essentially, describes the mechanism of ice failure by means of only three parameters: the brittle fracture strength of ice, the axial strain in ice at the final stage of failure, and the ice clearing stress magnitude, can be improved and extended. It seems that, first of all, an attempt of including the strain-rate dependence of the ice failure phenomena should be made. Further, the stochastic character of such quantities, as an impacting floe size and thickness, together with its velocity, could be considered, since in the present analysis all these quantities have been treated as deterministic variables. Hence, a full statistical analysis for a wide set of environmental parameters should, ideally, be carried out. These parameters include the probability distributions for the floe velocities, the floe diameters and thicknesses, and the frequency of floe impacts observed in a given area. Also, it would be highly advisable to measure the ice–structure contact stress histories in a series of individual impact events, but this part of observations is most difficult, and expensive, to perform. Having all the above-mentioned statistical data at disposal, and running the stochastic model with these data as input, exceedance probabilities of the extreme impact forces acting on an engineering structure can be generated, enabling in this way a proper risk assessment of the structure safety and reliability.

References

Ashby M. F., Hallam S. D. (1986), The failure of brittle solids containing small cracks under compressive stress-states, *Acta Metall.*, **34** (3), 497–510.

Hawkes I., Mellor M. (1972), Deformation and fracture of ice under uniaxial stress, *J. Glaciol.*, **11** (61), 103–131.

Hibler W. D. (1979), A dynamic thermodynamic sea ice model, *J. Phys. Oceanogr.*, **9** (4), 815–846.

Iliescu D., Schulson E. M. (2002), Brittle compressive failure of ice: monotonic versus cyclic loading, *Acta Mater.*, **50** (8), 2163–2172.

Ip C. F., Hibler W. D., Flato G. M. (1991), On the effect of rheology on seasonal sea-ice simulations, *Ann. Glaciol.* **15**, 17–25.

Jordaan I. J. (2001), Mechanics of ice–structure interaction, *Eng. Fract. Mech.*, **68** (17-18), 1923–1960.

Kamio Z., Matsushita H., Strnadel B. (2003), Statistical analysis of ice fracture characteristics, *Eng. Fract. Mech.*, **70** (15), 2075–2088.

Kim J., Shyam Sunder S. (1997), Statistical effects on the evolution of compliance and compressive fracture stress of ice, *Cold Reg. Sci. Technol.*, **26** (2), 137–152.

Morland L. W., Staroszczyk R. (1998), A material coordinate treatment of the sea-ice dynamics equations, *Proc. R. Soc. Lond.*, A **454** (1979), 2819–2857.

Nixon W. A. (1996), Wing crack models of the brittle compressive failure of ice, *Cold Reg. Sci. Technol.*, **24** (1), 41–55.

Overland J. E., Pease C. H. (1988), Modeling ice dynamics of coastal seas, *J. Geophys. Res.*, **93** (C12), 15,619–15,637.

Palmer A. C., Sanderson T. J. O. (1991), Fractal crushing of ice and brittle solids, *Proc. R. Soc. Lond.*, A **433**, 469–477.

Pralong A., Hutter K., Funk M. (2006), Anisotropic damage mechanics for viscoelastic ice, *Continuum Mech. Thermodyn.*, **17** (5), 387–408.

Sanderson T. J. O. (1988), *Ice Mechanics. Risks to Offshore Structures*. Graham and Trotman, London.

Schulson E. M., Gratz E. T. (1999), The brittle compressive failure of orthotropic ice under triaxial loading, *Acta Mater.*, **47** (3), 745–755.

Sjölind S. G. (1987), A constitutive model for ice as a damaging visco-elastic material, *Cold Reg. Sci. Technol.*, **14** (3), 247–262.

Smith R. B. (1983), A note on the constitutive law for sea ice, *J. Glaciol.*, **29** (101), 191–195.

Staroszczyk R. (2005), Loads exerted by floating ice on a cylindrical structure, *Arch. Hydroeng. Environ. Mech.*, **52** (1), 39–58.

Staroszczyk R. (2006), Loads exerted on a cylindrical structure by floating ice modelled as a viscous-plastic material, *Arch. Hydroeng. Environ. Mech.*, **53** (2), 105–126.

Tremblay L. B. (1999), A comparison study between two visco-plastic sea-ice models, [in:] *Advances in Cold-Region Thermal Engineering and Sciences* (eds. K. Hutter, Y. Wang and H. Beer), pp. 333–352, Springer, Berlin.

Xu Y., Xu J., Wang J. (2004), Fractal model for size effect on ice failure strength, *Cold Reg. Sci. Technol.*, **40** (1–2), 135–144.